Recent Results on B Meson Oscillations

SAU LAN WU

Physics Department, University of Wisconsin– Madison
Madison, WI, 53706, USA

Abstract

This paper presents recent time-dependent measurements of neutral B meson oscillations. Similar to the K^0–$\bar{K}^0$ system, there are two such systems involving the b quark: B_d^0–$\bar{B}_d^0$ and B_s^0–$\bar{B}_s^0$. Thus the physical states are respectively K_S and K_L, $(B_d)_S$ and $(B_d)_L$, and $(B_s)_S$ and $(B_s)_L$. The oscillation between each pair of states can be used to determine their mass difference. The present world average for the $(B_d)_S$–$(B_d)_L$ mass difference is $\Delta m_d = 0.457 \pm 0.019$ ps^{-1} (or $(3.01 \pm 0.13) \times 10^{-4}$ eV). Using $f_{B_s} = 12\%$ (the fraction of B_s produced in b events), the current lower limit on the corresponding Δm_s is 6.1 ps^{-1} (or 4.0×10^{-3} eV).

(Invited talk at the XVII International Symposium on
Lepton-Photon Interactions, Beijing, China, August 1995.)

Recent Results on B Meson Oscillations

SAU LAN WU

Physics Department, University of Wisconsin– Madison
Madison, WI, 53706, USA
E-mail: WUS@cernvm.cern.ch

ABSTRACT

This paper presents recent time-dependent measurements of neutral B meson oscillations. Similar to the K^0–$\bar{K}^0$ system, there are two such systems involving the b quark: B_d^0–$\bar{B}_d^0$ and B_s^0–$\bar{B}_s^0$. Thus the physical states are respectively K_S and K_L, $(B_d)_S$ and $(B_d)_L$, and $(B_s)_S$ and $(B_s)_L$. The oscillation between each pair of states can be used to determine their mass difference. The present world average for the $(B_d)_S$–$(B_d)_L$ mass difference is $\Delta m_d = 0.457\pm0.019$ ps^{-1} (or $(3.01\pm0.13)\times10^{-4}$ eV). Using $f_{B_s} = 12\%$ (the fraction of B_s produced in b events), the current lower limit on the corresponding Δm_s is 6.1 ps^{-1} (or 4.0×10^{-3} eV).

1. Introduction

Since there are three known quarks of charge $-\frac{1}{3}$, namely d, s and b, there are three similar neutral particle–antiparticle systems:

$$K^0(\bar{s}d)\text{–}\bar{K}^0(s\bar{d}), \quad B_d(\bar{b}d)\text{–}\bar{B}_d(b\bar{d}), \quad \text{and} \quad B_s(\bar{b}s)\text{–}\bar{B}_s(b\bar{s}).$$

Of these three, the K^0–$\bar{K}^0$ system is best measured experimentally[1,2] and understood theoretically[3]. However, the theoretical analysis applies equally well to all three cases.

As the topic here is the $B\bar{B}$ mixing, let B and $\bar{B}$ denote the flavor state in all three cases, i.e.,

$$\begin{aligned} B &= K^0 \quad B_d \quad or \quad B_s \\ and \quad \bar{B} &= \bar{K}^0 \quad \bar{B}_d \quad or \quad \bar{B}_s, \end{aligned}$$

while the corresponding weak eigenstates are

$$\begin{aligned} B_S &= K_S, \quad (B_d)_S \quad or \quad (B_s)_S \\ and \quad B_L &= K_L, \quad (B_d)_L \quad or \quad (B_s)_L. \end{aligned}$$

Because of CP non-conservation, B_S and B_L, which are not orthogonal, can most generally be related to B and $\bar{B}$ by

$$\begin{aligned} B_S &= \left(|p|^2 + |q|^2\right)^{-\frac{1}{2}} \left(pB + q\bar{B}\right) \\ and \quad B_L &= \left(|p|^2 + |q|^2\right)^{-\frac{1}{2}} \left(pB - q\bar{B}\right). \end{aligned}$$

Let $\Gamma = (\Gamma_S + \Gamma_L)/2$ and $m = (m_S + m_L)/2$ be the average width and mass of B_S and B_L, while $\Delta\Gamma$ and Δm are the differences

$$\Delta\Gamma = \Gamma_S - \Gamma_L > 0$$

and
$$\Delta m = |m_S - m_L|.$$

Let $\mathcal{P}_{B,u}(t)$ and $\mathcal{P}_{\bar{B},u}(t)$ be the probability distributions for a meson which is created as B (or $\bar{B}$) to decay as a B (or $\bar{B}$) after a proper time t, and $\mathcal{P}_{B,m}(t)$ and $\mathcal{P}_{\bar{B},m}(t)$ be those for a meson created as B (or $\bar{B}$) to decay as a $\bar{B}$ (or B), where the subscripts u and m stand for *unmixed* and *mixed* respectively. These four quantities are given by

$$\mathcal{P}_{B,u}(t) = \frac{|p|^2}{\Gamma\left[\frac{|p|^2+|q|^2}{\Gamma^2-(\Delta\Gamma/2)^2} + \frac{|p|^2-|q|^2}{\Gamma^2+(\Delta m)^2}\right]} e^{-\Gamma t}\left[\cosh\frac{\Delta\Gamma}{2}t + \cos\Delta m\,t\right]$$

$$\mathcal{P}_{B,m}(t) = \frac{|q|^2}{\Gamma\left[\frac{|p|^2+|q|^2}{\Gamma^2-(\Delta\Gamma/2)^2} + \frac{|p|^2-|q|^2}{\Gamma^2+(\Delta m)^2}\right]} e^{-\Gamma t}\left[\cosh\frac{\Delta\Gamma}{2}t - \cos\Delta m\,t\right]$$

$$\mathcal{P}_{\bar{B},u}(t) = \frac{|q|^2}{\Gamma\left[\frac{|p|^2+|q|^2}{\Gamma^2-(\Delta\Gamma/2)^2} - \frac{|p|^2-|q|^2}{\Gamma^2+(\Delta m)^2}\right]} e^{-\Gamma t}\left[\cosh\frac{\Delta\Gamma}{2}t + \cos\Delta m\,t\right]$$

$$\mathcal{P}_{\bar{B},m}(t) = \frac{|p|^2}{\Gamma\left[\frac{|p|^2+|q|^2}{\Gamma^2-(\Delta\Gamma/2)^2} - \frac{|p|^2-|q|^2}{\Gamma^2+(\Delta m)^2}\right]} e^{-\Gamma t}\left[\cosh\frac{\Delta\Gamma}{2}t - \cos\Delta m\,t\right]. \qquad (1)$$

Although these three systems, K^0–$\bar{K}^0$, B_d–$\bar{B}_d$, and B_s–$\bar{B}_s$ can be described by the same set of equations, the different decay modes lead to significant differences in the behavior of these systems. For K^0–$\bar{K}^0$, the $\pi\pi$ mode dominates with the immediate consequence that $\Gamma_S \gg \Gamma_L$; in fact,

$$\Gamma_S/\Gamma_L \sim 580.$$

In contrast, both B_d and B_s have many important decay modes. Indeed, for both cases the width difference $\Delta\Gamma$ comes from decay modes that are available to both B and $\bar{B}$. Using the many measured branching ratios for B_d, a generous estimate gives $(\Delta\Gamma/\Gamma)_d < 5\%$, perhaps much less. Since there is very little experimental information about the decay modes of B_s, no such firm statement can be made about the ratio $(\Delta\Gamma/\Gamma)_s$, but it is also believed to be small. In this talk, the width difference $\Delta\Gamma$ will be neglected for both the B_d–$\bar{B}_d$ and the B_s–$\bar{B}_s$ systems.

From Eq. (1), if the effect of CP non-conservation is neglected, then the formulas for the four probabilities simplify to

$$\begin{aligned}
\mathcal{P}_u(t) &= \mathcal{P}_{B,u}(t) = \mathcal{P}_{\bar{B},u}(t) = \frac{\Gamma^2-(\Delta\Gamma/2)^2}{2\Gamma}e^{-\Gamma t}\left[\cosh\frac{\Delta\Gamma}{2}t + \cos\Delta m\,t\right] \\
\mathcal{P}_m(t) &= \mathcal{P}_{B,m}(t) = \mathcal{P}_{\bar{B},m}(t) = \frac{\Gamma^2-(\Delta\Gamma/2)^2}{2\Gamma}e^{-\Gamma t}\left[\cosh\frac{\Delta\Gamma}{2}t - \cos\Delta m\,t\right].
\end{aligned} \qquad (2)$$

If, furthermore, $\Delta\Gamma$ is neglected, the preceeding equations can be written as

$$\mathcal{P}_u(t) = \frac{\Gamma}{2}e^{-\Gamma t}\left[1 + \cos\Delta m\,t\right]$$

$$\mathcal{P}_m(t) = \frac{\Gamma}{2}e^{-\Gamma t}\left[1 - \cos\Delta m\,t\right]. \qquad (3)$$

2

For the K^0–$\bar{K}^0$ system, the mass difference Δm was measured a long time ago[2] to be $3.51 \times 10^{-6} eV$. The purpose of this talk is to present and discuss recent experimental results on Δm_d and Δm_s for the B_d–$\bar{B}_d$ and B_s–$\bar{B}_s$ systems. The most sensitive measurements of Δm_d and Δm_s are obtained through *time-dependent* measurements, which investigate $\mathcal{P}_u$ and $\mathcal{P}_m$ directly, and this talk will consider only time-dependent measurements of these quantities. Since neither CP non-conservation nor the width differences $\Delta\Gamma$ have been observed in these systems, the analyses have been carried out on the basis of Eq. (3) rather than the more accurate Eqs. (1) or (2).

2. Experimental Overview

In order to perform a time-dependent measurement of Δm_d or Δm_s, one must measure the proper time of the decay of the B meson, and determine its *production flavor* (i.e., B or $\bar{B}$ at production) and *decay flavor* (i.e., B or $\bar{B}$ at decay) in order to ascertain whether the B meson is mixed or unmixed. The value of Δm is then found from the fraction of events identified (or *tagged*) as mixed or unmixed as a function of the measured proper time. Fig. 1 addresses the experimental sensitivity of such a measurement. Fig. 1(a), (b) and (c) each show the decay probabilities $\mathcal{P}_u(t)$ and $\mathcal{P}_m(t)$, discussed above. Each figure assumes a B lifetime of 1.5 ps, and shows the effect of different values of Δm on $\mathcal{P}_u(t)$ and $\mathcal{P}_m(t)$. Fig. 1(a) shows these probabilities for $\Delta m_d = 0.5$ ps^{-1}. It demonstrates that, since the typical experimental resolution for the LEP experiments is about 0.25 ps in B meson proper time, it is a relatively easy job to measure Δm_d due to the large oscillation period. Fig. 1(b) illustrates that if $\Delta m_s = 5$ ps^{-1}, the oscillation period is still within a comfortable reach of the experimental sensitivity. For $\Delta m_s = 15$ ps^{-1}, Fig. 1(c) shows that the experimental sensitivity for LEP experiments makes it difficult to extract the frequency of oscillation.

The proper time t of the B decay is obtained through

$$t = l\left(\frac{m_B}{p_B}\right) \tag{4}$$

where l is the decay *flight distance* between the B production point and decay point, and m_B and p_B are respectively the mass and momentum of the B meson. The flight distance is measured with the aid of silicon microvertex detectors which allow the production and decay vertices to be reconstructed precisely. The B meson decay length is determined by reconstructing a decay vertex formed from a lepton with high transverse momentum (or p_t) and a "charm track". The "charm track" is formed by combining information from several tracks which are not consistent with coming from the production point of the B and form a secondary "charm vertex". (In the case where a D^* from B decay is fully reconstructed, a variation of this method is used; see section 3.3). Because of the presence of tails in the flight distance resolution, it must
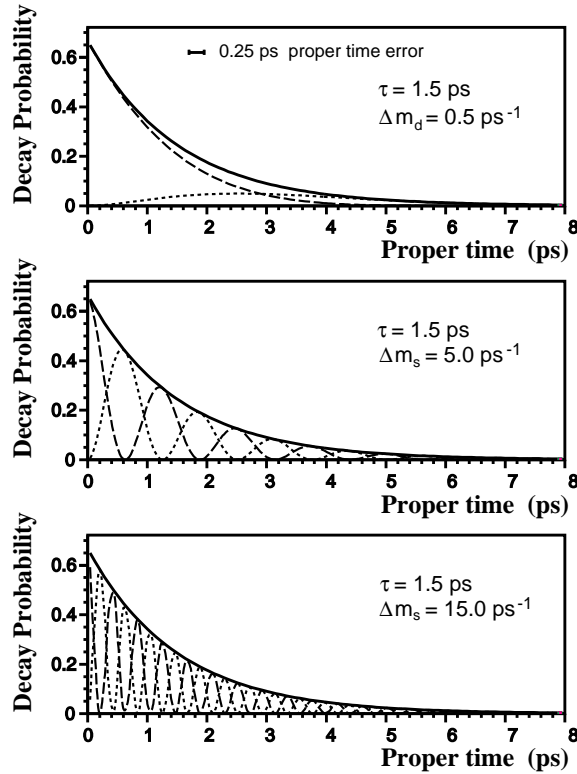
Fig. 1. $\mathcal{P}_u$ and $\mathcal{P}_m$ for (a) $\Delta m = 0.5$ ps^{-1}. (b) $\Delta m = 5$ ps^{-1}. (c) $\Delta m = 15$ ps^{-1}. The solid line shows the exponential decay of the B meson with a lifetime of 1.5 ps. The dashed line shows the $\mathcal{P}_u$ distribution, and the dotted line shows the $\mathcal{P}_m$ distribution.

be parametrized with several Gaussians. Typically half of the measurements fall in the "core", where the error is smallest. This core resolution is 260 μm for ALEPH[4], 340 μm for DELPHI[5], and 400 μm for OPAL[6].

The B momentum is obtained by reconstructing the momenta of the charged and neutral decay products of the B. The charged momentum can be reconstructed by simply summing the momenta of charged tracks consistent with coming from the decay of the B. These usually include a lepton and other charged tracks from a charm meson decay vertex. The neutral energy reconstruction is generally more complicated, involving information from the whole event, the beam energy, and energy-momentum conservation. The B momentum core resolution in ALEPH[7], DELPHI[5] and OPAL[6] is about 8–10%.

The charge of the b quark when it is created (the production flavor) is typically found in one of two ways. Some analyses require a lepton in the hemisphere opposite to the lepton used to determine the decay flavor, and use its sign to determine the production flavor. Others use *Jet charge* techniques, which weight momentum information from charged tracks in the event to determine the production flavor.

The charge of the b quark when it decays (the decay flavor) can be measured in a variety of ways. In some analyses, the sign of a high p_t lepton is used to identify the decay flavor. In other analyses, a $D^{*\pm}$ is reconstructed, and the sign of the $D^{*\pm}$ is used to determine the B_d^0 decay flavor.

Details of the specific methods used are discussed in the next section.

3. Measurement of Δm_d.

B_d oscillation was first observed by ALEPH[8] at LEP in 1993. Since then, a vast number of measurements have emerged using a variety of methods. The popular methods are described here, namely the "Lepton–Jet charge" method, the "Lepton–Lepton" method and methods using a D^*. The names of these methods are chosen such that the word before the hyphen refers to the way the decay flavor is determined, while that after the hyphen is for the corresponding production flavor.

3.1. Lepton–Jet charge Method.

In the Lepton–Jet charge method, events with semileptonic decay $b \to X\ell^-\bar{\nu}$ or $\bar{b} \to X\ell^+\nu$, ($\ell^\pm = e^\pm or \mu^\pm$) are selected with a high p_t lepton; the charge of the lepton from these decays identifies the decay flavor of the b quark. Leptons from other sources, particularly cascade decays $b \to c \to \ell^+$ dilute the sample of $b \to \ell^-$, but the high p_t lepton is nevertheless a good measure of the b decay flavor. The production flavor is then tagged by a Jet charge technique, discussed below. The B meson decay vertex is determined by the intersection of the high p_t lepton and the "charm track" on one side of the event, as described in section 2. The schematic of this method is shown in Fig. 2(a).

There are several different algorithms used to determine the b production flavor. The choice of charged tracks used in these analyses varies. ALEPH[7] and DELPHI[5] use only the tracks in the hemisphere opposite to the lepton, while OPAL[9] uses charged tracks from both the lepton jet, and the highest energy jet which does not contain the lepton, also called the *opposite side* jet, in calculating its jet charge. For convenience, this paper will refer to both jet charge and hemisphere charge measurements as jet charge measurements.

The weighting scheme for the ALEPH and DELPHI results takes the form

$$Q_H = \frac{\sum_{i=1}^{n_H} w_i q_i}{\sum_{i=1}^{n_H} w_i} \tag{5}$$

where n_H is the number of tracks in the opposite hemisphere, q_i is the charge of the track, and w_i is the weight used, taking the form $|\vec{p_i} \cdot \vec{e}|^\kappa$, where $\vec{e}$ is the direction of the thrust axis for ALEPH, and the direction of the sphericity axis for DELPHI. ALEPH calculates this weight using $\kappa = 0.5$, while DELPHI uses $\kappa = 0.6$. OPAL

5

uses a different jet charge, defined by

$$Q_{2J} = \sum_i q_i - 10 \sum_j q_j \left(\frac{p_{j\parallel}}{E_{\text{beam}}} \right) \tag{6}$$

where the first sum is over the tracks in the jet containing the high p_t lepton, and the second sum is over the opposite side jet. In Eq. (6), E_{beam} is the beam energy, and $p_{i\parallel}$ is the charged track's momentum parallel to its jet axis.

Because only one high p_t lepton is required, the "Lepton–Jet charge" method retains a relatively large sample of events and hence possesses a strong statistical power. The *tag rate*, or the fraction of events correctly identified as mixed or unmixed, for jet charge analyses is approximately 70% for both mixed and unmixed events. The ALEPH result studies the time dependence of the lepton-signed jet charge (jet charge multiplied by sign of lepton) distribution, without explicitly identifying events as mixed or unmixed. The results of Δm_d from ALEPH[7], DELPHI[5] and OPAL[9] using this method are shown in Figs. 2(b), 2(c) and 2(d). Throughout this report, where errors are given, the first is statistical and the second is systematic.

3.2. Lepton–Lepton Method

Dilepton measurements are in many ways similar to jet charge measurements. In the Lepton–Lepton method, events with semileptonic decay $b \to X \ell^- \bar{\nu}$ or $\bar{b} \to X \ell^+ \nu$, ($\ell^\pm = e^\pm$ or $\mu^\pm$), on both sides of the event are selected. The B meson decay vertex is determined by the intersection of the high p_t lepton and the "charm track" on one side of the event, as described in section 2. The B meson decay flavor is tagged by the sign of the high p_t lepton on the flight distance side of the event, just as in the Lepton–Jet charge method. The flavor at production time is tagged by a lepton in the opposite hemisphere. Contributions from mixing of the opposite side B hadron are independent of the proper time in the flight distance hemisphere, and their effect is factored into the tag rate calculation. The entire process can then be repeated with the roles of the leptons reversed, giving up to two measurements per event. The schematic of this method is shown in Fig. 3(a).

Because of the requirement that a lepton be found in each hemisphere, Lepton–Lepton measurements have a smaller event sample than Lepton–Jet charge analyses. Compensating for their smaller event sample, Lepton–Lepton analyses have superior tag rates, correctly identifying events as mixed or unmixed 80% of the time. This gives them sensitivity comparable to the Lepton–Jet charge method. The results from ALEPH[7], OPAL[6], and CDF[10] using this method are presented in Fig. 3(b), 3(c), and 3(d).
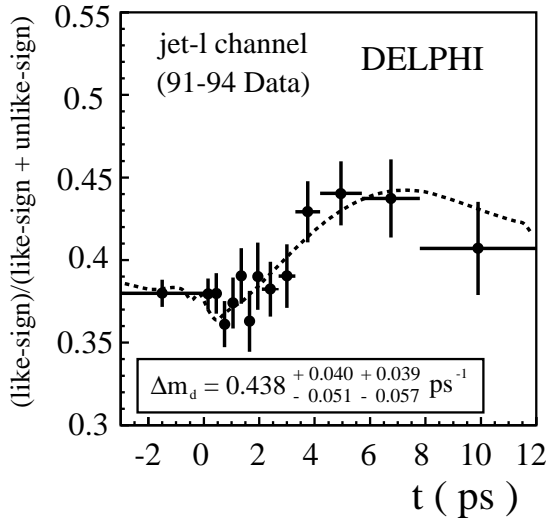
Using the Lepton–Lepton method, the DELPHI experiment[5] finds $\Delta m_d = 0.42 \pm 0.08^{+0.08}_{-0.07}$ ps^{-1}. DELPHI extends this method by including the use of a charged kaon to identify the decay flavor of the B meson, making use of DELPHI's unique feature,
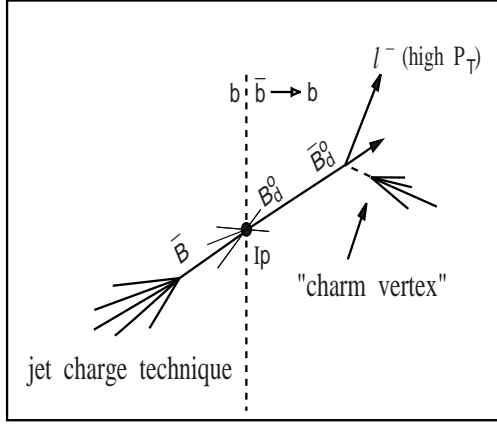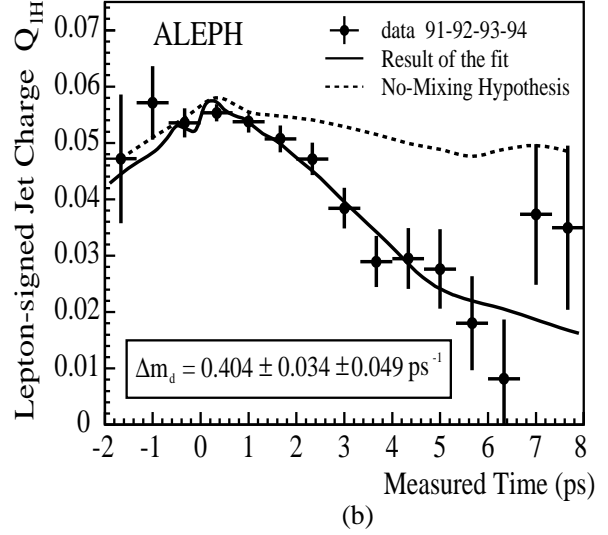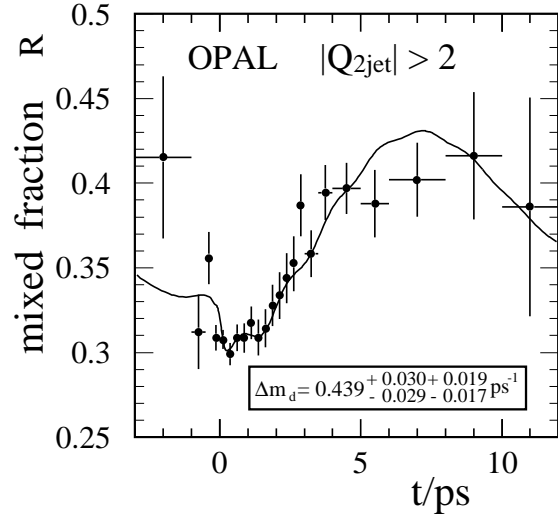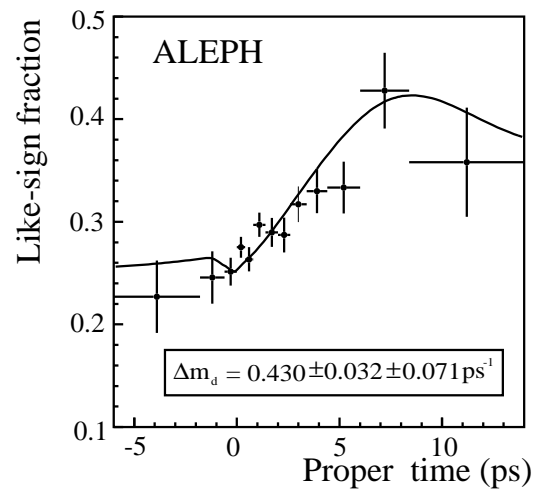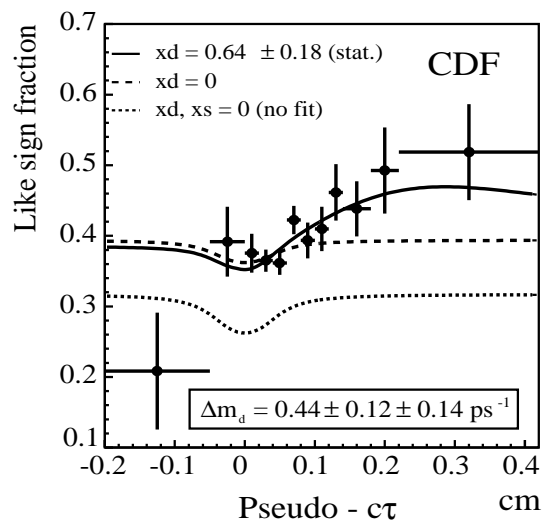
Fig. 2. Measurement of Δm_d with the Lepton–Jet charge method. (a) Schematic. (b) ALEPH measurement. (c) DELPHI measurement. (d) OPAL measurement.

7

Fig. 3. Measurement of Δm_d with the Lepton–Lepton method. (a) Schematic. (b) ALEPH measurement. (c) OPAL measurement. (d) CDF measurement.

the RICH counters. Thus, in the flight distance hemisphere, the measurement uses a lepton or a charged kaon coming from the secondary vertex, relying on the dominant decay chain $b \rightarrow c \rightarrow s$ to identify the B flavor. Such a kaon can be used in either the flight distance hemisphere to determine the decay flavor, or the opposite hemisphere, to determine the production flavor. This analysis also incorporates the jet charge or lepton in the opposite hemisphere to determine the production flavor. The DELPHI measurement using this Lepton–Kaon–Jet charge method[5] is $\Delta m_d = (0.563^{+0.050}_{-0.046} \pm 0.058)$ ps^{-1}. Because of the strong statistical correlation expected between this result and the other inclusive DELPHI results, it has not been included in the final Δm_d average given in Section 3.4.

3.3. Methods using a D^*.

It is also possible to carry out time-dependent measurements of Δm_d by reconstructing a $D^{*\pm}$ from the decay of a B meson. By selecting a charged D^* sample, it is possible to obtain a very pure sample of B_d mesons. Though some B^+ mesons contribute to the D^{*-} sample, the contamination is small, and the effect of these B^+ decays can be included in the fit for Δm_d. Because a D^* candidate must be reconstructed, these analyses typically have much smaller event samples than either the Lepton–Jet charge or the Lepton–Lepton measurements. Two methods are described here, the "D^*–Lepton or Jet charge" method, and the "D^* Lepton–Jet charge" method. The schematic for these methods is shown in Fig. 4(a).

In the D^*–Lepton or Jet charge analyses, a D^0 sample is reconstructed using the decays to $K\pi$, $K\pi\pi^0$, and $K\pi\pi\pi$. and then the D^0 is combined with a pion to produce a charged D^*. The decay flavor of the B_d is identified by the sign of this D^*. The production flavor can be identified with either a jet charge technique or with a lepton in the hemisphere opposite the D^*, as discussed in the previous sections. As the pion from the D^* decay has low momentum, and travels along the flight direction, it cannot be used to determine the B decay point. The apparent D^0 decay vertex is used to infer the B flight distance. The result from the ALEPH experiment[7] using the D^*–Lepton or Jet charge method is shown in Fig. 4(b). The DELPHI experiment[5] obtains $\Delta m_d = 0.470 \pm 0.086 \pm 0.061$ ps^{-1} with this method, while OPAL[11] finds $\Delta m_d = 0.57 \pm 0.11 \pm 0.02$ ps^{-1}.

In the D^* Lepton–Jet charge analyses, a D^* sample is produced as described above, and a lepton in the same hemisphere is used to form a B_d decay vertex, for measuring the flight distance. The decay flavor is determined by the sign of the D^*, and the production flavor is determined by a jet charge technique, as discussed in previous sections. The result from the DELPHI D^* Lepton–Jet charge analysis[5] is shown in Fig. 4(c), while the OPAL result[12] is shown in Fig. 4(d). DELPHI has performed
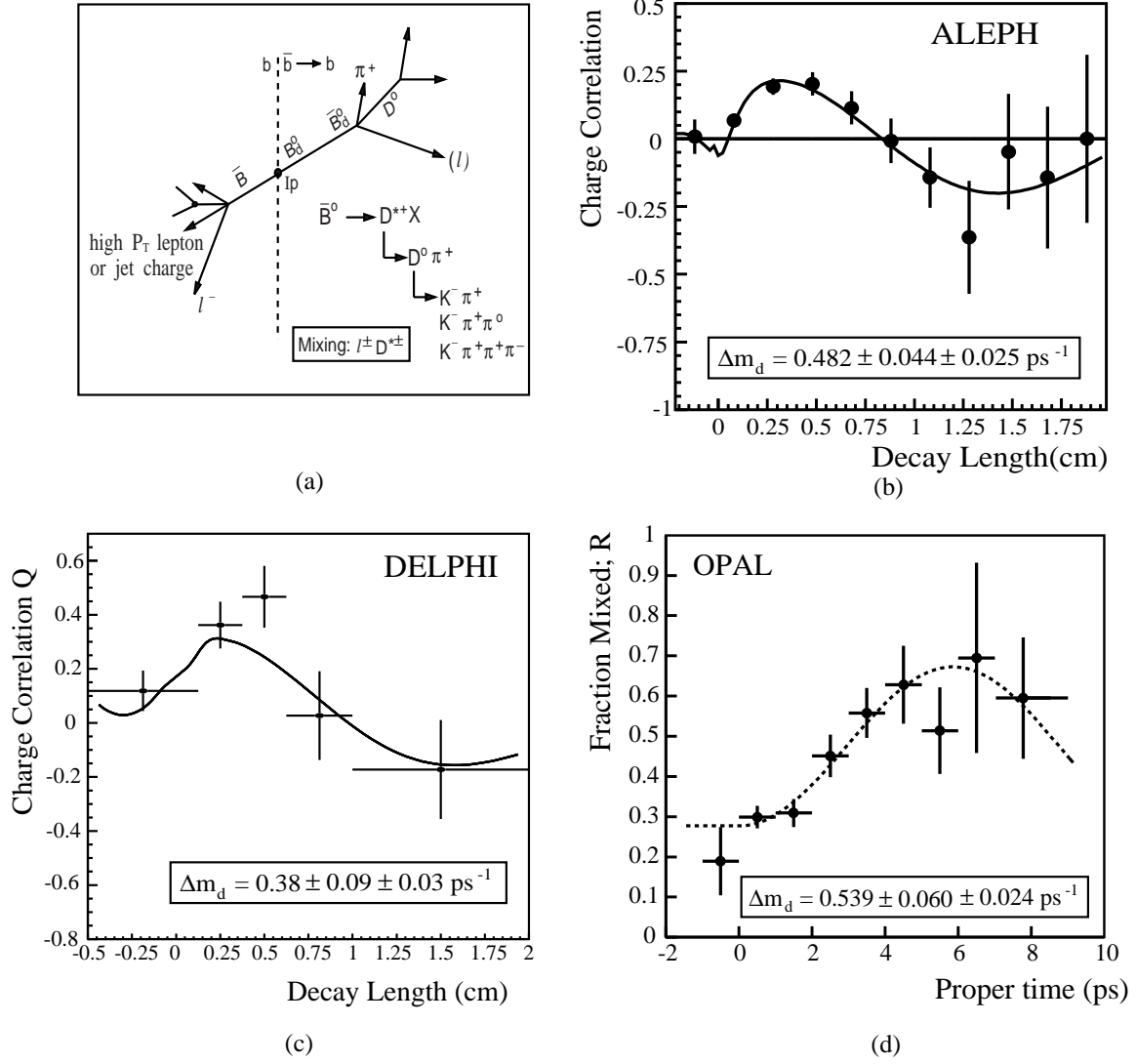
Fig. 4. Measurement of Δm_d with the D^* methods. (a) Schematic. (b) ALEPH D^*–Lepton or Jet charge measurement. (c) DELPHI D^* Lepton–Jet charge measurement. (d) OPAL D^* Lepton–Jet charge measurement.

The combined D^* based result from DELPHI is $\Delta m_d = 0.421 \pm 0.064 \pm 0.042$ ps^{-1}.

an average of their D^* based analyses[5], giving $\Delta m_d = (0.421 \pm 0.064 \pm 0.042)$ ps^{-1}, which has been included in the LEP and world averages computed in Section 3.4.

3.4. Average of Δm_d Results.

The process of performing an average on the measurements of Δm_d is complicated by the presence of correlations between the various measurements. These correlations can be *statistical*, coming from overlapping data samples, or *systematic*, coming from common assumptions used in making the measurement.

Where measurements are statistically correlated, the degree of correlation is generally unknown. To minimize correlations, when there have been multiple measurements of similar types performed on the same data sample, the average includes only those results with the smallest errors. Where measurements are systematically correlated, it is possible to judge the degree of correlation between different results by looking at common correlated systematic errors.

The main correlated systematic errors come from the lifetimes and fractions of individual B hadron species. Thus, the averaging process considers correlations related to the lifetimes and fractions only. There are other errors which are correlated, in theory, such as the parametrization of the b fragmentation function, and the decay length resolution in individual LEP experiments, but these errors are generally smaller, and their correlations can safely be neglected.
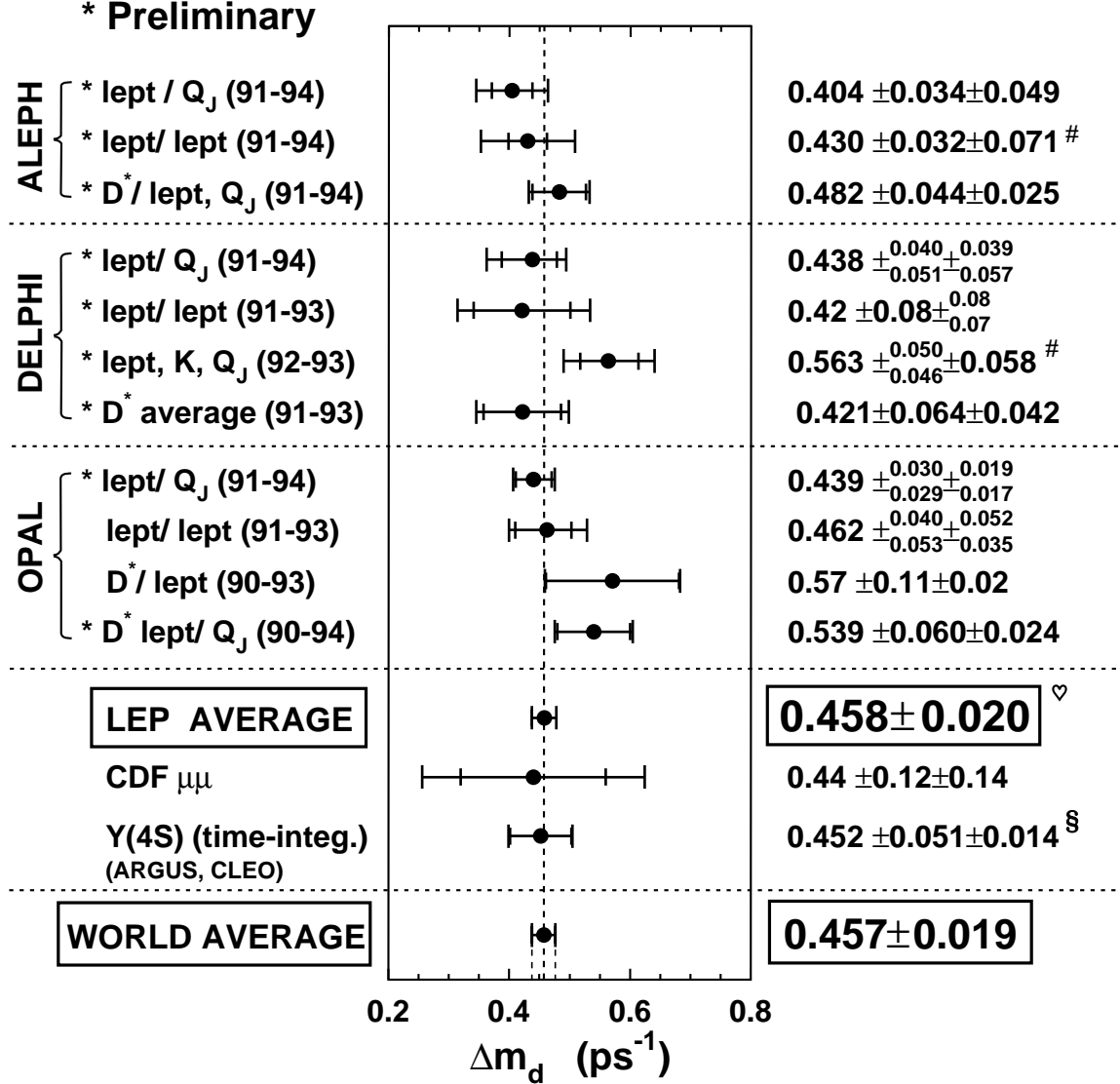
Taking these correlations into account correctly is complicated by the fact that each measurement parametrizes these systematic effects in a different way, and use different central values and errors on their parameters. The average considers the individual parametrizations of these different experiments, and performs a constrained fit[13] for Δm_d, the lifetimes and the B hadron fractions.

Using this averaging technique, and excluding the ALEPH lepton–lepton measurement and the DELPHI Lepton–Kaon–Jet charge measurement due to statistical overlap, the LEP average is found to be $\Delta m_d = 0.458 \pm 0.020$ ps^{-1}. Including results from CDF and time integrated measurements from $\Upsilon(4s)$ in the average yields $\Delta m_d = 0.457 \pm 0.019$ ps^{-1}. A summary of the results is presented in Fig. 5.

4. Measurement of Δm_s.

Both Δm_d and Δm_s are mass differences between particles and hence they are of direct physical importance. A further motivation for measuring these quantities comes from the fact that these mass differences are due to high-order weak interactions. The important diagrams for these interactions are shown in Fig. 6 together with similar diagrams with the W and top quark lines exchanged. Computation from

Summary of Δm_d Results

* Preliminary

ALEPH	* lept / Q$_J$ (91-94)	0.404 ±0.034±0.049
	* lept/ lept (91-94)	0.430 ±0.032±0.071 [#]
	* D*/ lept, Q$_J$ (91-94)	0.482 ±0.044±0.025
DELPHI	* lept/ Q$_J$ (91-94)	0.438 $+^{0.040}_{0.051}+^{0.039}_{0.057}$
	* lept/ lept (91-93)	0.42 ±0.08$+^{0.08}_{0.07}$
	* lept, K, Q$_J$ (92-93)	0.563 $+^{0.050}_{0.046}$±0.058 [#]
	* D* average (91-93)	0.421±0.064±0.042
OPAL	* lept/ Q$_J$ (91-94)	0.439 $+^{0.030}_{0.029}+^{0.019}_{0.017}$
	lept/ lept (91-93)	0.462 $+^{0.040}_{0.053}+^{0.052}_{0.035}$
	D*/ lept (90-93)	0.57 ±0.11±0.02
	* D* lept/ Q$_J$ (90-94)	0.539 ±0.060±0.024
	LEP AVERAGE	**0.458± 0.020** [♡]
	CDF $\mu\mu$	0.44 ±0.12±0.14
	Y(4S) (time-integ.) (ARGUS, CLEO)	0.452 ±0.051±0.014 [§]
	WORLD AVERAGE	**0.457±0.019**

$\Delta m_d \quad (ps^{-1})$

 # Not used for average (due to statistical correlation)

§ τ_{B° = 1.57± 0.05 ps is used

♡ LEP average calculated with correlated and anticorrelated errors; constraints are applied to the B fractions and b hadron lifetimes (Thanks to H-G Moser).
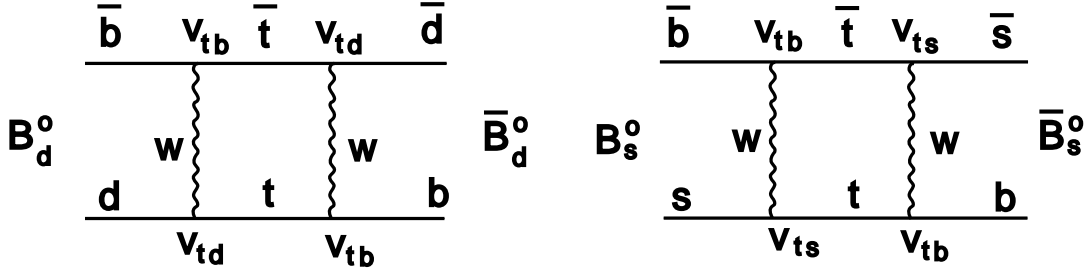
Fig. 5. Summary of results for Δm_d.

12

Fig. 6. Important quark diagrams (including those with W and top quark lines exchanged) for the calculation of Δm_d and Δm_{s}.

these diagrams gives

$$\frac{\Delta m_{\mathrm{s}}}{\Delta m_d} \simeq \frac{m_{B_{\mathrm{s}}}}{m_{B_d}} \left|\frac{V_{ts}}{V_{td}}\right|^2 \xi_{\mathrm{s}}^2 \frac{\hat{\eta}_{B_{\mathrm{s}}}}{\hat{\eta}_{B_d}} \tag{7}$$

where $\hat{\eta}_{B_{\mathrm{s}}}$ and $\hat{\eta}_{B_d}$ are the QCD correction factors for the B_{s} and B_d, expected to be similar, and ξ_{s} is the ratio of hadronic matrix elements for the B_{s} and B_d. Estimates from lattice QCD[14] and QCD sum rules[15] are consistent with a value[16] of $\xi_{\mathrm{s}} = 1.16 \pm 0.10$. Measurements of Δm_d and Δm_{s} can therefore be used to determine $|V_{ts}/V_{td}|$. This ratio of the CKM matrix elements is of special interest because it appears in one of the most useful unitarity triangles given by

$$\frac{V_{td}}{V_{ts}} + V_{us}^* + \frac{V_{ub}^*}{V_{ts}} = 0. \tag{8}$$

For a number of reasons, the measurement of Δm_{s} is much more difficult than that for Δm_d. The theoretical expectation that Δm_{s} is significantly larger than Δm_d has been confirmed by experiments[6,17]. As illustrated in Fig. 1, such larger values of Δm_{s} lead to rapid oscillation, which complicates the measurement. A second difficulty comes from the fact that $f_{B_{\mathrm{s}}}$, the fraction of B_{s} produced in b decays, is substantially smaller than f_{B_d} and is not well measured.

Three methods for determination of Δm_{s} will be described here. They are the "Lepton–Jet charge" method, the "Lepton–Lepton" method and the "Lepton–Kaon Correlation" method.

4.1. Lepton–Jet charge Method

This method has been used by the ALEPH[4], DELPHI[5], and OPAL[9] collaborations at LEP, and its schematic is that of Fig. 2(a) with B_d and $\bar{B}_d$ replaced by B_{s} and $\bar{B}_{\mathrm{s}}$. Again, the B decay vertex is formed by the secondary vertex including a high p_t
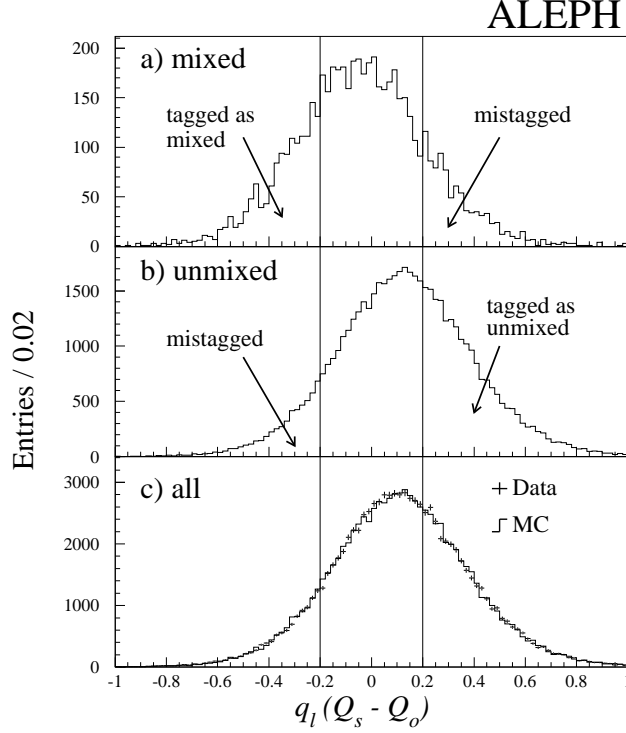
Fig. 7. Lepton signed same side minus opposite side jet charge distributions for a) mixed B^0 mesons, and b) unmixed b hadrons in the full Monte Carlo simulation. Plotted in c) is the sum of all Monte Carlo events, normalized to the number of events in the data. The data points are superimposed with error bars. The vertical lines indicate the selection requirement $|Q_S - Q_O| > 0.2$.

lepton. The decay flavor is tagged by the high p_t lepton while the production flavor is tagged by the jet charge technique.

Since the lower bound from ALEPH[4] using this method is the best one for Δm_s, it will be described in detail here. The main difference between the ALEPH Lepton–Jet charge method for Δm_s and that for Δm_d described in Sec. 3.1 is that a different jet charge algorithm is used. Instead of using the Q_H in Eq. (5) where only the charged tracks in the opposite hemisphere are used, the new jet charge algorithm makes use of information from both the opposite jet and the flight distance jet. The weight applied to each track in computing the jet charge value for the event is the track's rapidity with respect to the jet axis. More precisely, define

$$Q_{S,O} = \frac{\sum_i y_i q_i}{\sum_i y_i} \qquad (9)$$

where S and O indicate the sum is over tracks in the same side jet (the jet with the high p_t lepton) and opposite side jet, respectively. The rapidity, y_i, is given by

$$y_i = \frac{1}{2} \ln \frac{E_i + P_{i\parallel}}{E_i - P_{i\parallel}}. \qquad (10)$$
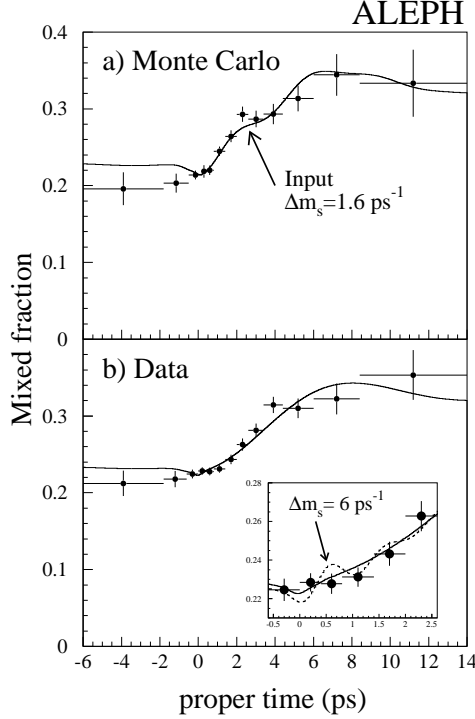
14

Fig. 8. The tagged mixed fraction of events as a function of measured proper time, for a) Monte Carlo with $\Delta m_s = 1.6$ ps^{-1}, and b) data events. The superimposed curve for the Monte Carlo in a) is the expected distribution for $\Delta m_s = 1.6$ ps^{-1}. The solid curve for the data in b) assumes $\Delta m_s = 30$ ps^{-1}, while the dashed curve in the insert is the expected distribution for $\Delta m_s = 6$ ps^{-1}. The small proper time region of the plot is expanded to emphasize the part most sensitive to B_s oscillations.

The jet charge variable used to identify the production flavor is then

$$Q = Q_S - Q_O. \tag{11}$$

For the purpose of tagging mixed or unmixed events, the charge q_ℓ of the high p_t lepton and the sign of the above Q are used. Events are identified as follows:

$$+ - \quad , \quad - + \quad \longleftrightarrow \quad \textit{mixed events}$$
$$+ + \quad , \quad - - \quad \longleftrightarrow \quad \textit{unmixed events}$$

As shown in Fig. 7, a cut requiring $|q_\ell \cdot Q| > 0.2$ is imposed. With this cut, the tag rate for unmixed events, A_u, is about 80% and for mixed events, A_m, is about 60%. Since there are eight times more unmixed events than mixed events, it is essential to have a high tag rate for unmixed events. This is a great advantage of using the Q defined in Eq. (11). To make optimal use of the experimental data, the method of maximum likelihood is used to extract the value of Δm_s.

Fig. 8 shows the tagged mixed fraction for Monte Carlo and data. The value of Δm_d is determined as a check of the tag rates used in this analysis, and of the
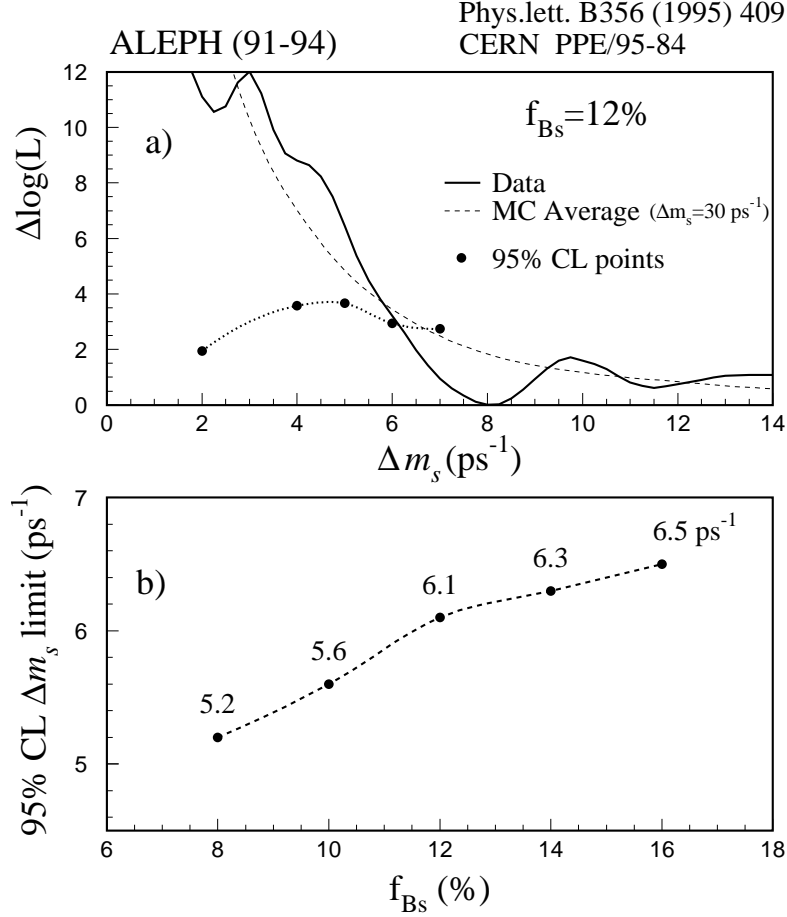
15

Fig. 9. Superimposed on the data likelihood curve are the average of the fast Monte Carlo $\Delta \log L$ values, and the 95% confidence limit points. $\Delta \log L$ is defined as the $(-\log L)$ value at the Δm_{s} value, minus the minimum $(-\log L)$ value. A limit curve is drawn through the 95% confidence limit points. The data curve crosses the limit curve at $\Delta m_{\mathrm{s}} = 6.1$ ps^{-1} for B_{s} fraction $f_{B_{\mathrm{s}}} = 12\%$. Also shown is the average of the $\Delta \log L$ curves for 200 fast Monte Carlo samples in which B_{s} mixing is near-maximal ($\Delta m_{\mathrm{s}} = 30$ ps^{-1}). b) the results of 95% confidence level limit in Δm_{s} as a function of the B_{s} fraction $f_{B_{\mathrm{s}}}$. The limits for Δm_{s} are 5.2, 5.6, 6.1, 6.3, and 6.5 for $f_{B_{\mathrm{s}}} = 8\%$, 10%, 12%, 14% and 16%, respectively.
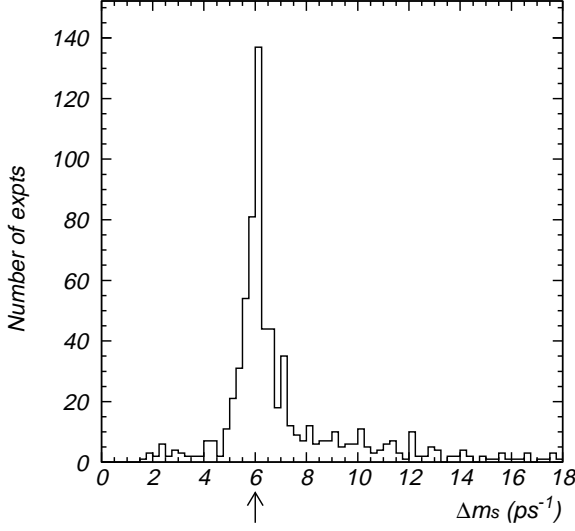
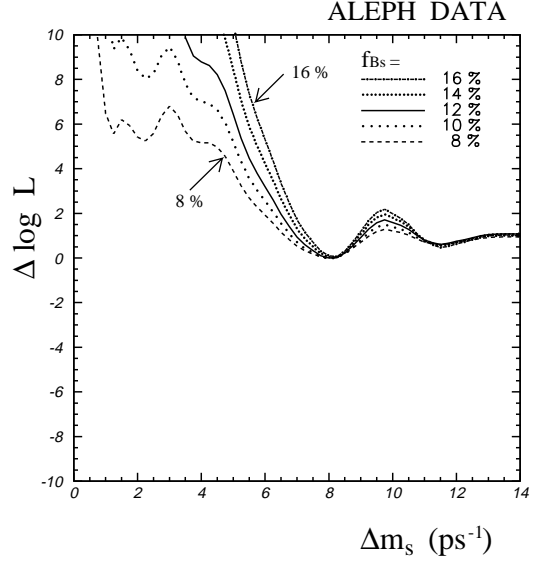Fig. 10. The likelihood minima for an input $\Delta m_{\mathrm{s}} = 6$ ps^{-1}.

Fig. 11. ALEPH data curve for different values of $f_{B_{\mathrm{s}}}$.

peformance of the likelihood fit. Assuming a B meson lifetime, τ_B, of 1.5 ps, B_d fraction, f_{B_d}, of 0.4, B_{s} fraction, $f_{B_{\mathrm{s}}}$, of 0.12, Δm_{s} of 30 ps^{-1}, and A_m of 0.6, a two-dimensional fit with the ALEPH data is performed for Δm_d and A_u. This gives $A_u = 0.792 \pm 0.003$ and $\Delta m_d = 0.47 \pm 0.04$ ps^{-1}, the latter value being in agreement with the world average of Fig. 5. Similar fits with Monte Carlo give $A_u = 0.792 \pm 0.003$ and $\Delta m_d = 0.48 \pm 0.05$ ps^{-1} to be compared with the input values of 0.790 and 0.467 ps^{-1} respectively.

The ALEPH result is shown in Fig. 9. This figure shows the $\Delta \log L$ curve for the data as a function of Δm_{s}, where $\Delta \log L$ is defined as the negative log likelihood value $(-\log L)$ at a given Δm_{s} minus the $(-\log L)$ value calculated at the Δm_{s} where the $(-\log L)$ is at its minimum. It uses the values of A_u and Δm_d determined above as inputs to the fit, and assumes a B_{s} fraction of $f_{B_{\mathrm{s}}} = 12\%$. The data prefer high values of Δm_{s}, with a favored value of 8 ps^{-1}. The difference in likelihood for higher values of Δm_{s} is insufficient to exclude them, therefore a lower limit is set on Δm_{s}. Superimposed on the data is a 95% confidence level lower limit curve calculated using a 'fast' Monte Carlo.

In constructing the limit curve, the likelihood differences, $\Delta \log L$, for the fast Monte Carlo are calculated for 300 samples at various input values of Δm_{s} (2.0, 4.0, 5.0, 6.0 and 7.0 ps^{-1}), each with sample size equal to that of the data. If the Δm_{s} value is close to the point where the limit is set, 600 samples are used. The 95% confidence limit is determined by locating the point below which lie 95% of the $\Delta \log L$ values, calculated at the input value of Δm_{s}. The 95% confidence limit curve is then drawn through the points at different input Δm_{s}, as shown in Fig. 9(a). The

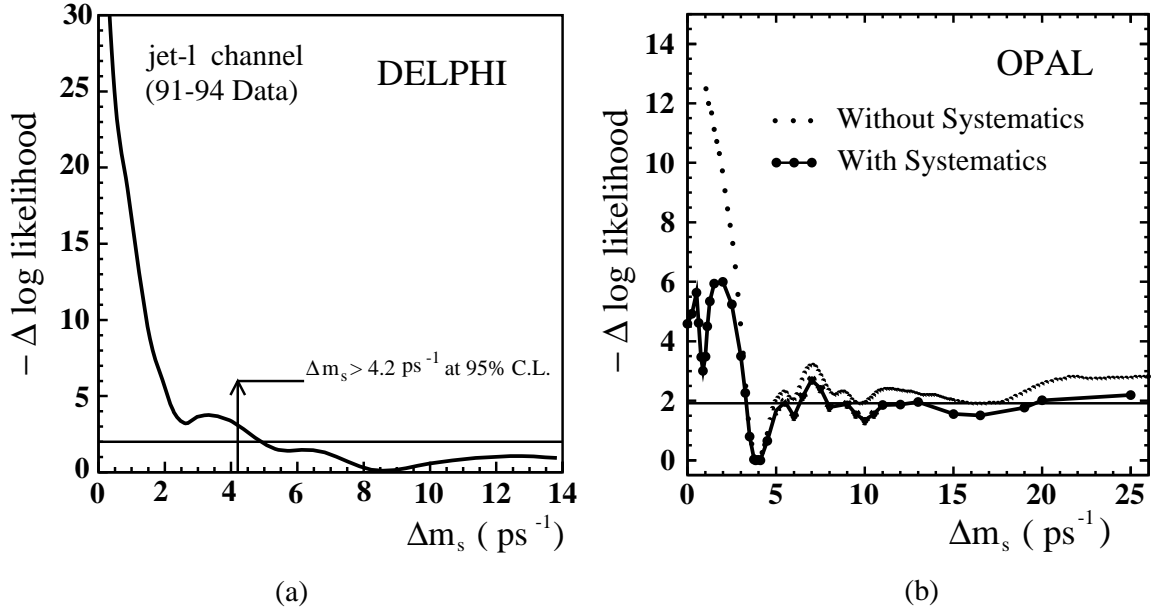Fig. 12. Limit on Δm_{s} from (a) DELPHI and (b) OPAL Lepton–Jet charge method.

data $\Delta \log L$ curve intersects the limit curve at $\Delta m_{\mathrm{s}} = 6.1$ ps^{-1}. This point is taken as the 95% confidence level lower limit. The lower plot of Fig. 9(b) shows the result of performing this complete analysis with several different values of $f_{B_{\mathrm{s}}}$ as discussed later in this section.

It is important to check that there is indeed sensitivity at $\Delta m_{\mathrm{s}} = 6$ ps^{-1}. For this purpose, 800 Monte Carlo samples were generated at this value of Δm_{s} with the statistics of each sample again matching those of the ALEPH data. For each of these 800 samples, the value of Δm_{s} at the minimum of the $(-\log L)$ curve is determined. The distribution of these minima are shown in Fig. 10. The figure clearly shows that in the majority of cases, the method does find the correct minimum, which demonstrates that there is indeed sensitivity at $\Delta m_{\mathrm{s}} = 6$ ps^{-1}.

The data curve of Fig. 9(a) corresponds to an input $f_{B_{\mathrm{s}}}$ of 12%. Fig. 11 shows the corresponding data curves obtained from the ALEPH data for various assumed B_{s} fractions. The figure demonstrates that the sensitivity to Δm_{s} increases as $f_{B_{\mathrm{s}}}$ increases. Fig. 9(b) shows the results of 95% confidence level lower limit in Δm_{s} as a function of $f_{B_{\mathrm{s}}}$. The limit varies from $\Delta m_{\mathrm{s}} > 5.2$ ps^{-1} at $f_{B_{\mathrm{s}}} = 8\%$ to $\Delta m_{\mathrm{s}} > 6.5$ ps^{-1} at $f_{B_{\mathrm{s}}} = 16\%$.

The corresponding preliminary results using the Lepton–Jet charge method from DELPHI[5] and OPAL[9] are shown in Fig 12. The result from DELPHI is $\Delta m_{\mathrm{s}} > 4.2$ ps^{-1} at 95% Confidence Level for $f_{B_{\mathrm{s}}} = (10 \pm 3)\%$, while from OPAL, the result is $\Delta m_{\mathrm{s}} > 3.3$ ps^{-1} at 95% Confidence Level for $f_{B_{\mathrm{s}}} = (12 \pm 3.6)\%$. Taking the data curve in Fig. 12(b) literally, OPAL also excludes ranges of Δm_{s} between 6.3 and
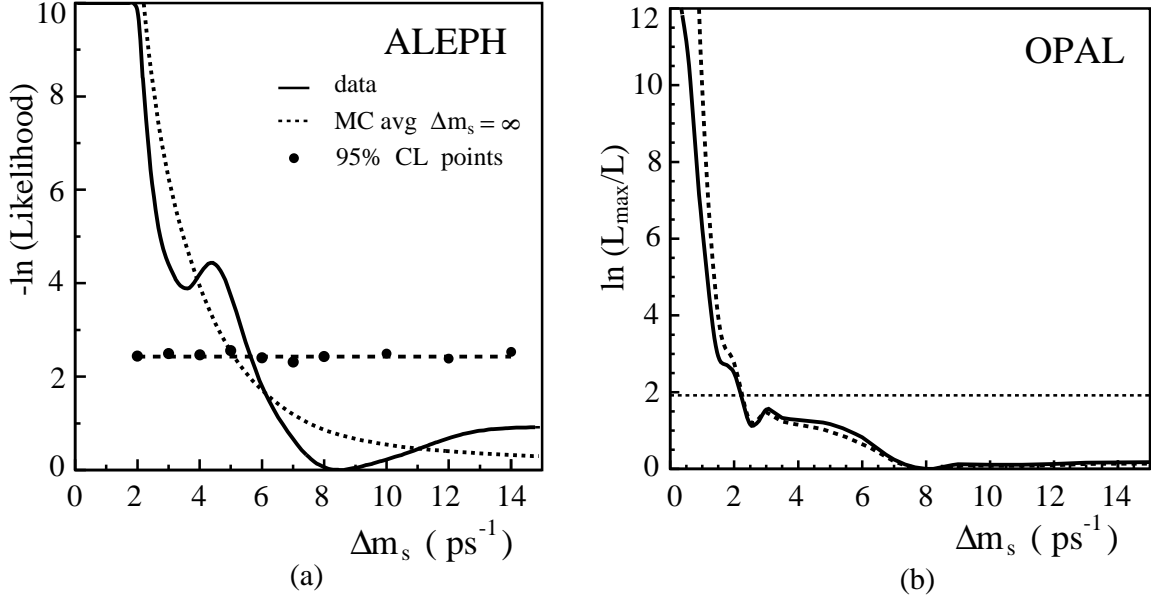
Fig. 13. Limit on $\Delta m_{\rm s}$ from (a) ALEPH and (b) OPAL Lepton–Lepton method.

7.9 ps^{-1} and above 19.6 ps^{-1} at 95% Confidence Level. At 97% Confidence Level, however, these exclusions disappear, so their significance is marginal.

4.2. Lepton–Lepton Method

This method has been used by the ALEPH[7] and OPAL[6] collaborations at LEP, and its schematic is that of Fig. 3(a) with the B_d and $\bar{B}_d$ replaced by $B_{\rm s}$ and $\bar{B}_{\rm s}$. As with the B_d analysis, the B decay vertex is formed by the secondary vertex including a high p_t lepton, and the decay and production flavors are tagged by the signs of leptons on the flight distance and opposite sides. The results from the ALEPH and OPAL collaborations are shown in Fig. 13. The preliminary result from ALEPH[7] is $\Delta m_{\rm s} > 5.6$ ps^{-1} at 95% Confidence Level for $f_{B_{\rm s}} = (12.2 \pm 3.2)\%$ while the published result from OPAL[6] is $\Delta m_{\rm s} > 2.2$ ps^{-1} at 95% Confidence Level for $f_{B_{\rm s}} = (12.0 \pm 3.6)\%$.

4.3. Lepton–Kaon Correlations Method

This method has been used by the ALEPH[18] collaboration, and its schematic is given in Fig. 14(a). In order to enrich the sample with $B_{\rm s}$ events, the analysis requires that a charged kaon from the primary vertex be identified. This kaon must have the opposite sign of the lepton or jet charge in the opposite hemisphere, in order to improve the tag of the production flavor. To enrich the decay vertex with $D_{\rm s}$, the "charm vertex" is required to contain either zero or two kaons, or one kaon with a
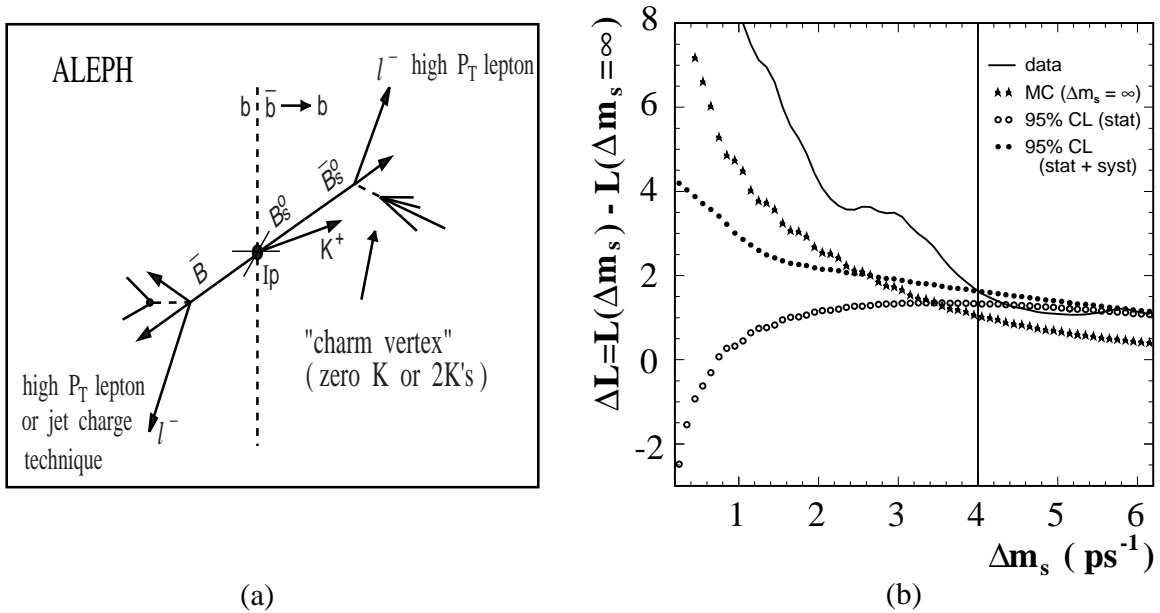
Fig. 14. Limit on Δm_s from ALEPH with Lepton–Kaon Correlations method.

charge opposite to the lepton. The decay flavor is tagged by the sign of the lepton from the decaying B meson, as in other methods.

This selection yields 4436 lepton–kaon correlations, and enriches the B_s sample by a factor of 1.35. The method has a high tag rate of about 80%. The preliminary result for this measurement is shown in Fig. 14(b) giving $\Delta m_s > 4.0\,\mathrm{ps}^{-1}$ at 95% Confidence Level for $f_{B_s} = (12 \pm 3)\%$.

4.4. Estimation of B_s fraction in b events.

There are currently two methods for determining the fraction of B_s in an inclusive lepton sample. The first method is from $D_s\ell$ correlations. ALEPH has measured the product branching ratio[19]:

$$f_{B_s} \cdot \mathrm{Br}(B_s^0 \to D_s^- \ell^+ \nu X) = 0.82 \pm 0.09(stat)^{+0.13}_{-0.14}(syst)\% \qquad (12)$$

and from this, derives[19,20] $f_{B_s} = 11.0 \pm 2.8\%$.

The second method uses the average time-integrated mixing parameter $\bar{\chi} = f_{B_s}\chi_s + f_{B_d}\chi_d$. Assuming $f_{B_u} + f_{B_d} + f_{B_s} + f_{\Lambda_b} = 1$, $f_{B_u} = f_{B_d}$, and $\chi_s = 0.5$, the B_s fraction is given by:

$$f_{B_s} = \frac{2\bar{\chi} - (1 - f_{\Lambda_b})\chi_d}{1 - \chi_d}. \qquad (13)$$

Using[21] $\tau_{B_d} = 1.570 \pm 0.049$ ps, $\Delta m_d = 0.458 \pm 0.020$ from the LEP average as given in Fig. 5, and the $\Upsilon(4s)$ average[22] $\chi_d(\Upsilon(4s)) = 0.167 \pm 0.025$, the world average of

Table 1. Summary of measurements of $\bar{\chi}$.

Measurement	$\bar{\chi}$
LEP+SLD[23] (dileptons)	0.1145 ± 0.0061
CDF (eμ)[24]	$0.118 \pm 0.008 \pm 0.020$
CDF ($\mu\mu$)[24]	$0.118 \pm 0.021 \pm 0.026$
D0 ($\mu\mu$)[25]	$0.09 \pm 0.04 \pm 0.03$
World Average	0.115 ± 0.006

the time-integrated B_d oscillation parameter, χ_d is calculated to be 0.170 ± 0.011. Table 1 gives the average mixing parameter, $\bar{\chi} = 0.115 \pm 0.006$. The baryon fraction, f_{Λ_b}, is derived from Λ_c–lepton and Λ–lepton correlations, in analogy with Eq. (12) above. Using[2] $Br(\Lambda_c \to \Lambda X) = 35 \pm 11\%$, the LEP measurements[26] can be averaged to yield

$$f_{\Lambda_b} \cdot Br(\Lambda_b \to \Lambda_c X \ell \nu) = 1.67 \pm 0.30\%, \qquad (14)$$

with common systematic effects taken into account. Following the method given in Ref. 20, the baryon fraction is then calculated to be $f_{\Lambda_b} = 12.8 \pm 3.9\%$.

With these inputs, f_{B_s} from the second method is then $9.9 \pm 1.9\%$. An average of the two methods then yields a final estimate of the fraction of B_s mesons produced in $Z \to b\bar{b}$ decay, $f_{B_s} = 10.2 \pm 1.6\%$.

4.5. Summary of lower limit for Δm_s

Table 2 summarizes the lower limits at 95% Confidence Level placed on Δm_s from the LEP experiments. These limits on Δm_s are computed using different techniques, and there is currently no combined result which takes correlated statistical and systematic errors into account. Thus, the best limits on B_s oscillation, $\Delta m_s > 6.1$ ps^{-1} for $f_{B_s} = 12\%$ and $\Delta m_s > 5.6$ ps^{-1} for $f_{B_s} = 10\%$ using the Lepton–Jet charge method by ALEPH are taken as the current limits on Δm_s. Defining $x_s = \Delta m_s \tau_{B_s}$ where[21] $\tau_{B_s} = 1.58 \pm 0.10$ ps^{-1}, the values of x_s are shown in Table 3 by shifting the central value of τ_{B_s} down by 1σ. Using the world average central values[16] of the quantities in Eq. (7) and including their uncertainties by shifting the values by 1σ to the conservative side, yields the ratios $\Delta m_s / \Delta m_d$ and $|V_{ts}/V_{td}|$ as shown in Table 3.

Table 2. Summary of Limits on $\Delta m_{\rm s}$ at 95% C.L.

	$\Delta m_{\rm s}$ (ps^{-1})	$f_{B_{\rm s}}$
ALEPH (91-94)	> 6.1	12%
(lept/Q$_J$)	> 5.6	10%
ALEPH (91-94)	> 5.6	12±3%
(lept/lept)		
ALEPH (91-94)	> 4.0	12±3%
(lept/K+Q_J)		
DELPHI (91-94)	> 4.2	10±3%
(lept/Q$_J$)		
DELPHI	> 1.5	
($D_{\rm s}\ell$/Q$_J$)		
OPAL (91-94)	> 3.3	12.0±3.6%
(lept/Q$_J$)		
OPAL (91-93)	> 2.2	12.0±3.6%
(lept/lept)		

Table 3. Constraints on physical quantities resulting from measurements of Δm_d and $\Delta m_{\rm s}$.

	$f_{B_{\rm s}} = 12\%$	$f_{B_{\rm s}} = 10\%$
$\Delta m_{\rm s}$	> 6.1 ps^{-1}	> 5.6 ps^{-1}
$x_{\rm s}$	> 9.0	> 8.3
$\Delta m_{\rm s}/\Delta m_d$	> 12.8	> 11.8
$|V_{ts}/V_{td}|$	> 2.8	> 2.7

5. Conclusion

In summary, by studying the time-dependence of B^0–$\bar{B}^0$ oscillations, recent experiments have given

(i) an accurate value for Δm_d, the mass difference between $(B_d)_L$ and $(B_d)_S$; and

(ii) a lower bound for $\Delta m_{\rm s}$, the mass difference between $(B_{\rm s})_L$ and $(B_{\rm s})_S$.

The results from the ALEPH, DELPHI and OPAL Collaborations at LEP of CERN and the CDF Collaboration at the Tevatron Collider of Fermilab are summarized in Table 4. In particular,

$$\frac{\Delta m_d}{\Delta m_K} = 85.8 \pm 3.6. \tag{15}$$

The impact of the results presented here is shown in Fig. 15 in the $(\Delta m_d, \Delta m_{\rm s})$ plane together with the region allowed by the Standard Model[27].

22

Table 4. Summary of Δm_d and Δm_s results.

Mass Differences for the Long and Short Eigenstates		
	Δm (ps^{-1})	Δm (eV)
Δm_K	$(5.33 \pm 0.03) \times 10^{-3}$	$(3.51 \pm 0.02) \times 10^{-6}$
Δm_d	0.457 ± 0.019	$(3.01 \pm 0.13) \times 10^{-4}$
Δm_s (95% C.L.) $f_{B_s} = 12\%$ $f_{B_s} = 10\%$	> 6.1 > 5.6	$> 4.0 \times 10^{-3}$ $> 3.7 \times 10^{-3}$
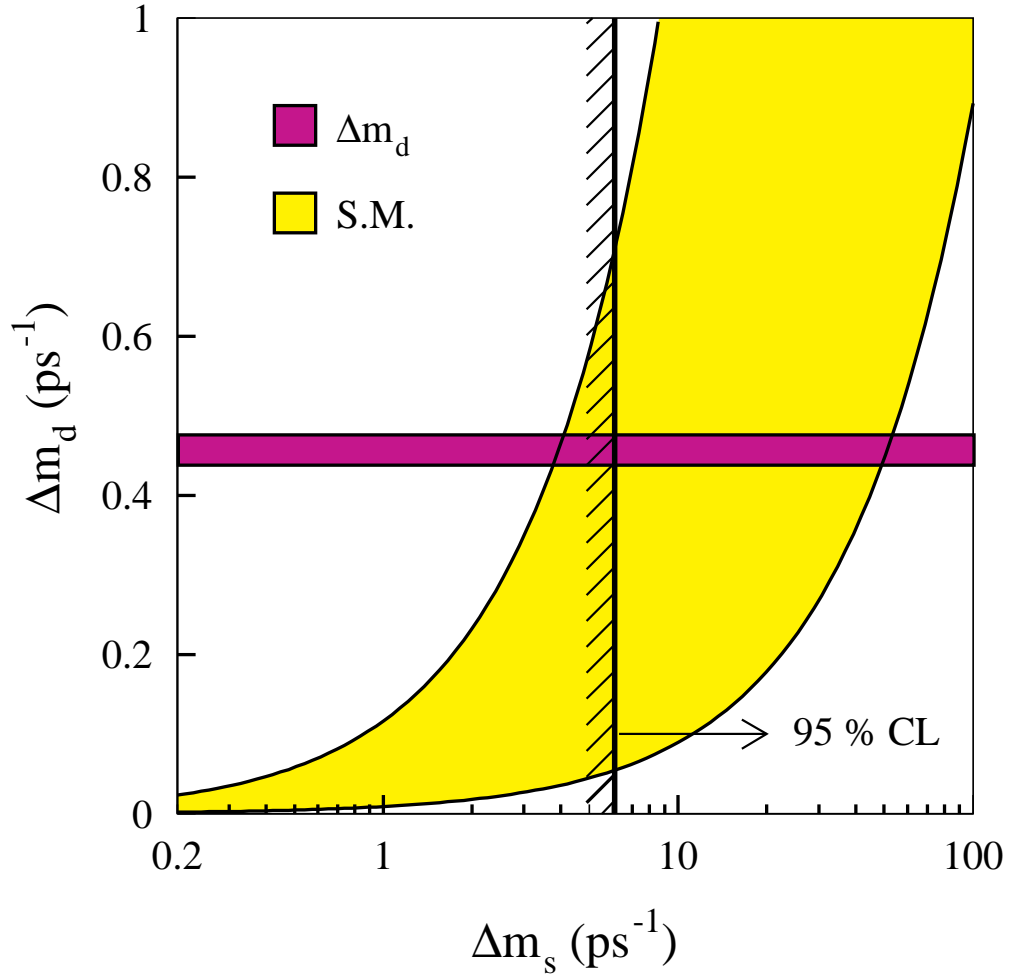
Fig. 15. Constraints on the $(\Delta m_d, \Delta m_s)$ plane.

23

6. Acknowledgement

7. References

1. J. H. Christenson, J. W. Cronin, V. L. Fitch, and R. Turlay, *Phys. Rev. Lett.* **13**, (1964) 138.
2. Review of particle properties, *Phys. Rev.* **D50** (1994) 1173.
3. T.T. Wu and C.N. Yang, *Phys Rev. Lett.* **13**, (1964) 380.
4. D. Buskulic *et al.* (ALEPH Collab.), *Phys. Lett.* **B356** (1995) 409.
5. DELPHI Collaboration, Improved Measurement of the Oscillation Frequencies of B^0 Mesons, contribution to this conference.
6. R. Akers *et al.* (OPAL Collab.), *Z. Phys.* **C66** (1995) 555.
7. ALEPH Collaboration, Measurement of the B_d^0–$\bar{B}_d^0$ Oscillation Frequency, contribution to this conference.
8. D. Buskulic *et al.* (ALEPH Collab.), *Phys. Lett.* **B313** (1993) 498.
9. OPAL Collaboration, A Study of B Meson Oscillations Using Inclusive Lepton Events, contribution to this conference.
10. CDF Collaboration, Measurement of $B^0\bar{B}^0$ Mixing via Time Evolution, contribution to this conference.
11. R. Akers *et al.* (OPAL Collab.), *Phys. Lett.* **B336** (1994) 585.
12. OPAL Collaboration, Update of the Measurement of the B_d^0 Oscillation Frequency Using a Jet Charge Technique, contribution to this conference.
13. This technique was developed by H.-G. Moser.
14. J. Shigemitsu, Lattice Gauge Theory : Status Report 1994. Proc. of XXVII Int. Conf. on High Energy Physics, Glasgow, July, 1994., Vol I, 135.
15. S. Narison, Precise Determination of f_{P_s}/f_P and Measurement of the "Perturbative" Pole Mass from f_P, *Phys. Lett.* **B322** (1994) 247;
S. Narison and A. Pivovarov, *Phys. Lett.* **B327** (1994) 341.
16. A. Ali and D. London, *Z. Phys.* **C65** (1995) 431.;
A. Ali and D. London, CP Violation and Flavour Mixing in the Standard Model, contribution to this conference.
17. D. Buskulic *et al.* (ALEPH Collab.), *Phys. Lett.* **B322** (1994) 441.

18. ALEPH Collaboration, Time Dependent B_{s} Mixing from Lepton-Kaon Correlations with the ALEPH Detector, contribution to this conference.

19. D. Buskulic *et al.* (ALEPH Collab.), Measurement of the B_{s}^0 Lifetime and Production Rate with $D_{\mathrm{s}}^-\ell^+$ Combinations in Z Decays, CERN-PPE/95-125, 1995.

20. D. Buskulic *et al.* (ALEPH Collab.), A Measurement of $|V_{cb}|$ from $\bar{B}^0 \to D^{*+}\ell^-\bar{\nu}_\ell$, CERN-PPE/95-94, 1995.

21. J. Kroll. Talk given in this conference.

22. P. Wells. Talk given in the International Europhysics Conference on High Energy Physics, Brussels, 1995.

23. Private communication from the LEP Electroweak Working Group;
P. Perret. Talk given in the International Europhysics Conference on High Energy Physics, Brussels, 1995.

24. CDF Collaboration, Measurement of the $B\bar{B}$ Mixing Parameter $\bar{\chi}$ at CDF, contribution to this conference.

25. D0 Collaboration, Measurement of B^0–$\bar{B}^0$ Mixing Using Dimuons at D0, contribution to this conference.

26. P. Abreu *et al.* (DELPHI Collab.), Lifetime and Production Rate of Beauty Baryons from Z Decays, CERN-PPE/95-054.
D. Buskulic *et al.* (ALEPH Collab.), Measurements of the b Baryon Lifetime, CERN-PPE/95-065.
R. Akers *et al.* (OPAL Collab.), Measurement of the Average b–Baryon Lifetime and the Product Branching Ratio $f(b \to \Lambda_b)\mathrm{BR}(\Lambda_b \to \Lambda\ell^-\bar{\nu}X)$, CERN-PPE/95-090.

27. This plot was initiated by R. Forty, Proc. of XXVII Int. Conf. on High Energy Physics, Glasgow, July, 1994., Vol. I, 171.
The allowed region from the Standard Model is given by Ref. 16 of Ali and London to be $10.3(\xi_{\mathrm{s}}/1.16)^2 \leq \Delta m_{\mathrm{s}}/\Delta m_d \leq 94.9(\xi_{\mathrm{s}}/1.16)^2$